Characteristics of Internal Inductively Coupled Plasma Source for Ultralarge-Area Plasma Processing

Characteristics of Internal Inductively Coupled Plasma Source for Ultralarge-Area Plasma Processing

Jong Hyeuk Lim, Gwang Ho Gweon, Seung Pyo Hong, Kyong Nam Kim, Yi Yeon Kim, and Geun Young Yeom

Department of Materials Science and Engineering, Sungkyunkwan University, Suwon, Kyunggi-do 440-746, Korea

Received December 2, 2009; accepted January 7, 2010; published online March 5, 2010

The capacitive–inductive (E–H) mode transition characteristics of an ultralarge-area (2,750 × 2,350 mm²) inductively coupled plasma (ICP) system with multiple internal U-type antennas have been investigated. When the electrical characteristics of the ICP antenna such as power transfer efficiency and ICP source impedance, were measured as a function of ICP power, a distinctive change from E to H mode was identified at an rf power of approximately 3 kW. When the power transfer mode was changed from capacitive to inductive for the multiple U-type antenna configuration, better plasma uniformity was obtained owing to the more uniform power deposition along the antenna line.

DOI: 10.1143/JJAP.49.030213

For the application to thin-film devices utilizing glass substrates or plastic substrates such as thin-film solar cells, flat-panel-display devices, and flexible display devices, high-density plasma sources such as very high frequency (VHF) capacitively coupled plasma and inductively coupled plasma (ICP) sources, have been investigated for faster material processing at lower substrate temperatures. In these devices, owing to the substrate dimensions of larger than 1 m, achieving a highly uniform plasma over the substrate surface is essential. Among the various high-density plasma sources, ICP sources are more easily extendable to a large size; therefore, they have been investigated as possible high-density plasma sources for the application to next-generation flat-panel displays. One of the most promising features of ICP sources is the mode transition, which relates the coupling characteristics to the plasma.[1,2] It is known that the capacitive (E) mode generates strong electrostatic coupling at a low rf power and the inductive (H) mode generates electromagnetic coupling at a high power. In particular, the transition region between the E-mode (electrostatic coupling) and H-mode (electromagnetic coupling) strongly depends on the plasma impedance and geometric parameters such as the discharge volume, the configuration of the inductive coil, and the power transferrd to the plasma.[3–5] The appropriate characteristic of the mode transition is very important for efficient plasma processing. In the case of ICP sources, when a low input power is applied to the ICP source antenna, capacitive coupling to the plasma with a low power transfer efficiency and unstable impedance matching can result.

In this study, the electrical characteristics and plasma characteristics of an ultralarge-area (2,750 × 2,350 mm²) ICP source with internal multiple U-type antennas were studied and their relation to the E–H mode change of the plasma source was investigated. To obtain more efficient inductive coupling, an ICP source antenna covered with a ferrite module was used. A previous study showed that, by covering the antenna line with semicircular a half-circle-type ferrite module, the internal-type ICP source exhibits more stable and higher-density plasmas below the antenna line through the reinforcement of the induced magnetic field below the antenna line and by preventing the loss of the magnetic field above the antenna line, which is close to the chamber top.[6]

The experimental setup of the internal ICP system used in this study is schematically shown in Fig. 1(a). The processing chamber has a rectangular shape with a size

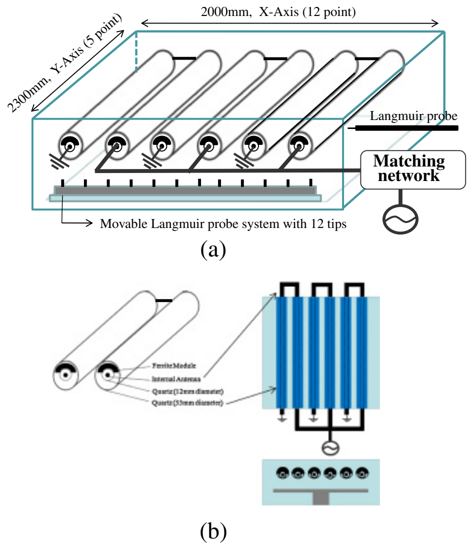

Fig. 1. (Color online) (a) Schematic diagram of the ICP system (2,750 × 2,350 mm³) with multiple U-type antennas used in the experiment. (b) Internal U-type antenna with a ferrite module and shielded with quartz tubing.

of 2,750 × 2,350 mm² for the application of large-area flat-panel-display processing and the substrate size was 2,300 × 2,000 mm². In the processing chamber, three pairs of U-type antennas were connected in parallel and one side of the antennas was connected to an 8 kW 2 MHz rf power generator through an L-type matching network while the other side was directly connected to the ground. Figure 1(b) shows one of the multiple U-type antennas. The antenna was made of 10-mm-diameter copper tubing for water cooling, and the outside of the antenna was coaxially covered by 33-mm-diameter quartz tubing to isolate the antenna and vacuum. A half-circle-shaped Ni–Zn ferrite module with a magnetic permeability of 500 covered the top of the antenna line to enhance the inductive field below the antenna line. In addition, to protect the ferrite module, another 12-mm-diameter quartz tube was located between the antenna and the ferrite module as shown in the figure. Because the 33-mm-diameter quartz tube separated the vacuum from the antenna, the inside of the 33-mm-diameter quartz tube was under atmospheric pressure, and the 12-mm-diameter quartz tube, which covered the ferrite module, was also under atmospheric pressure. A Langmuir probe (Hiden Analytical ESP) was installed 5 cm below the antenna and at the *Y*-axis

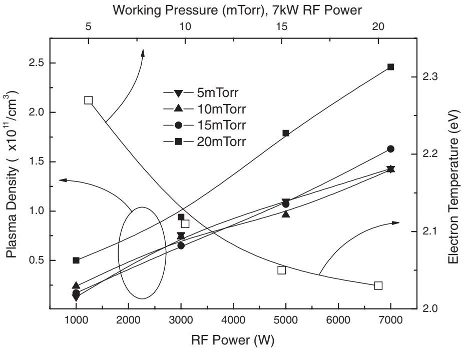

(a)

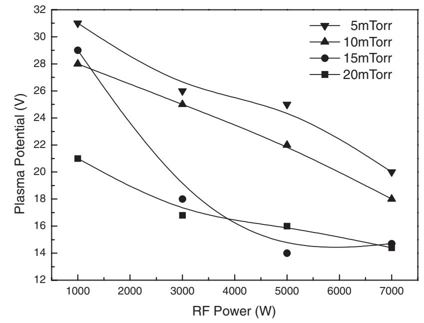

(b)

Fig. 2. (a) Ar^+ ion density and electron temperature and (b) plasma potential measured by a Langmuir probe 5 cm below the antenna as a function of rf ICP power at various operating Ar pressures.

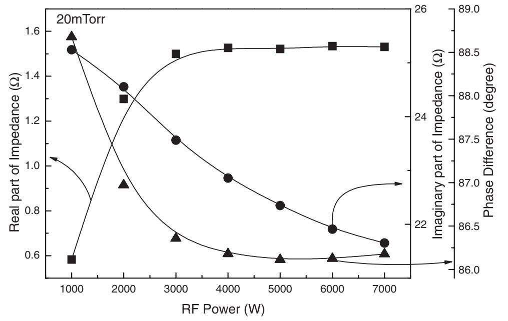

(a)

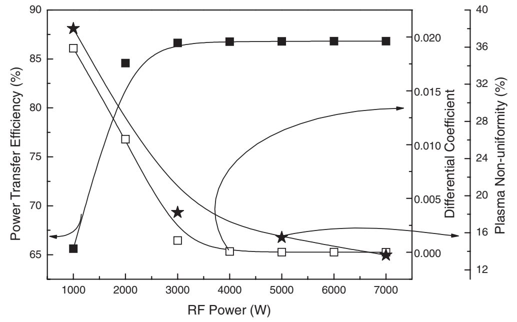

(b)

Fig. 3. (a) Real and imaginary parts of impedance and the phase difference of the internal-type ICP source measured by an impedance analyzer located between the matching box and the antenna. (b) Power transfer efficiency and its derivatives as a function of rf ICP power at 20 mTorr Ar calculated using the data obtained from the impedance analyzer. The plasma nonuniformity measured over the substrate area ($2{,}300 \times 2{,}000\,mm^2$) as a function of rf ICP power at 20 mTorr Ar is also shown.

center of the chamber as shown in Fig. 1(a). In addition, to estimate the plasma uniformity over the large-area substrate, a home-made scanning Langmuir probe system composed of 12 probe tips located 32 cm below the antenna line, aligned across the antenna line, and separated by an equal distance of 15 cm was installed in the chamber as shown in Fig. 1(a). Moreovers, by biasing the probe tips at −40 V, the ion saturation currents, along and perpendicular to the antenna line were measured while moving the probe system in the chamber. The electrical properties of the internal ICP source antenna were measured by an impedance analyzer (MKS) located between the matching box and the antenna.

Figure 2(a) shows the plasma density and electron temperature of the large-size internal-type ICP measured using a Langmuir probe as a function of rf power at the Y-axis center of the chamber as shown in Fig. 1(a). As shown in the Fig. 2(a), as the rf power was increased from 1 to 7 kW, the plasma density increased almost linearly. In the case of 20 mTorr Ar gas and an rf power of 7 kW, a high-density plasma with a density of about $2.5 \times 10^{11}\,cm^{-3}$ was obtained. The electron temperatures were generally low for the operating conditions used in this experiment and, as shown in Fig. 2(a), for an ICP power of 7 kW, an increase in operating pressure from 5 to 20 mTorr decreased the electron temperature slightly from 2.3 to 2.0 eV, although the variation of the electron temperature was not significant. As shown in Fig. 2(b), the plasma potential generally decreased with increasing of rf power and operating pressure.

Generally, for a conventional ICP, with increasing of rf power, abrupt changes in the plasma coupling mode from a low-density E-mode to a high-density H-mode can be seen from the changes in the plasma parameters such as plasma density and electron temperature. However, in this experiment with an internal multiple U-type ICP having a ferrite module, no abrupt jump of the plasma density was observed. Most researchers who have studied the E–H transition have investigated the phenomena of transitions using external-type ICP systems.[1,3,7] The lack of abrupt in changes plasma density observed in our internal-type ICP might be related to the different configuration of the ICP source antenna used in our system. Although the plasma parameters did not show significant evidence of an E–H mode transition with increasing rf ICP power, the decrease in plasma potential and increase in plasma density with increasing rf ICP power are believed to be related to the transition of the power transfer mode from capacitive coupling to inductive coupling.

To observe the change of the power transfer mode more clearly, the electrical characteristics of the rf ICP source were measured using an impedance analyzer in the case of 20 mTorr Ar and the results such as the real and imaginary parts of impedance, and the phase angle between voltage and current measured as a function of rf ICP power are shown in Fig. 3(a). As shown in Fig. 3(a), with increasing rf ICP power from 1 to 7 kW, the real part of the impedance (load resistance) was increased from 0.58 to about 1.53 Ω while the imaginary part of the impedance (load reactance) decreased from 25.2 to 21.6 Ω, indicating an increase in the power transfer efficiency with increasing of rf ICP power. The phase angle between the voltage and current decreased from 88.6 to 86.1° with increasing rf ICP. The increase in the real part of the impedance and the decrease in the

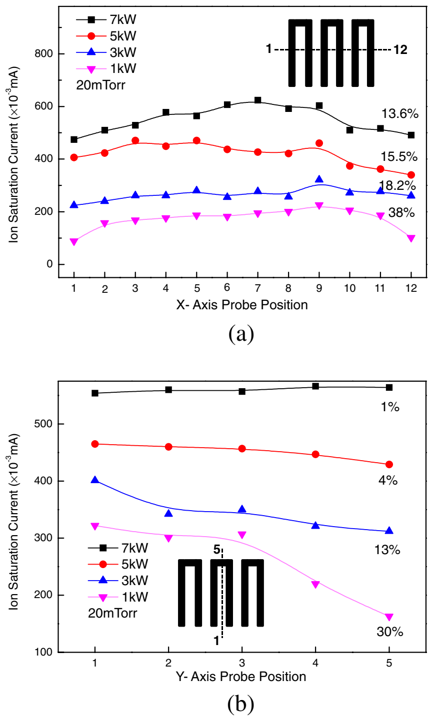

Fig. 4. (Color online) Ion saturation current measured along the horizontal centerline direction (a) and vertical centerline direction (b) of the processing chamber at 20 mTorr Ar as a function of rf ICP power.

imaginary part of the impedance with increasing rf ICP power indicate an increase in the mutual inductive coupling between the antenna and plasma.[8,9] In particular, the significant changes in the real part of the impedance and the phase angle observed between rf ICP powers of 1 and 3 kW may be related to the change in the power transfer mode from the inefficient capacitive mode to the efficient inductive mode.

The power transfer efficiency (ε) was calculated from the relationship among the input power to the antenna (P_{input}), the rf rms current, and the resistance:[10,11)]

$$\frac{P_{input} - I_{rf}^{2}R}{P_{input}} \times 100.$$

Here, $I_{rf}^{2}R$ ($P_{Joule\ Loss} = I^{2}_{rf} \times R$) is the Joule loss consumed by the antenna with the ferrite module. As shown in Fig. 3(b), the power transfer efficiency was increased from 65 to 87% with increasing rf ICP power from 1 to 7 kW and the significant change in the power transfer efficiency between 1 and 3 kW indicated the change in the power transfer mode from E to H.

Figures 4(a) and 4(b) show the ion saturation current measured along the horizontal centerline direction (a) and vertical centerline direction (b) of the processing chamber at 20 mTorr Ar as a function of rf ICP power. As shown in Figs. 4(a) and 4(b), with increasing rf ICP power, the uniformities of the ion saturation currents measured along both the horizontal direction and the vertical direction were improved from 38 to 13.56% for the horizontal direction and from 30 to 1% for the vertical direction with increasing of rf ICP power from 1 to 7 kW.

In the case of the ion saturation current measured along the horizontal direction shown in Fig. 4(a), the improvement

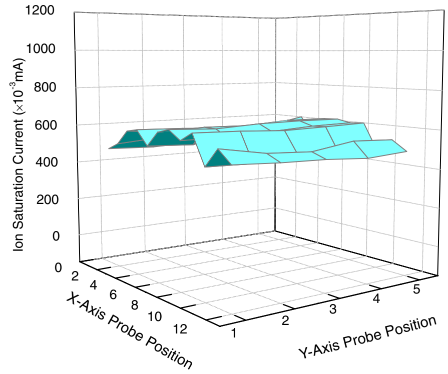

Fig. 5. (Color online) Ion saturation current measured over the entire substrate surface (2,300 x 2,000 mm^2) for 20 mTorr Ar and 7 kW rf ICP power (plasma uniformity is 13.6%).

in the uniformity with increasing rf ICP power was due to the decreased loss of ions to the chamber wall with increasing plasma density.[12)] In the case of the ion saturation current measured along the vertical direction shown in Fig. 4(b), at the lower rf ICP power, position 1 (near the power input and ground) exhibited a higher ion saturation current than position 5 (near the center position of the U-type connection). Also, a brighter plasma was observed near position 1 than near position 5. However, as the rf ICP power is increased to higher than 3 kW, owing to the increase in inductive coupling, which causes the power transfer to the plasma along all of the antenna line by the antenna current, a more uniform plasma is believed to be obtained. In Fig. 5, the ion saturation current measured over the entire surface is shown for 20 mTorr Ar and an rf ICP power of 7 kW. The plasma uniformity was 13.6% as shown in Fig. 3(b). In the internal U-type antenna, the change from capacitive coupling (E-mode) to inductive coupling (H-mode) improved the plasma uniformity significantly by removing the local capacitively coupled discharge caused by the antenna voltage differences between the U-type antenna ends. At 20 mTorr Ar and 7 an rf ICP power of 7 kW, a plasma uniformity of 13.6% with a plasma density of about 2.5×10^{11} cm^{-3} was obtained over the substrate (2,300 × 2,000 mm^2). Furthers improvement in the plasma uniformity with a higher plasma density is expected to be achieved by applying a higher rf ICP power to the ICP source.

Acknowledgment This work was supported by the "Development Program of Nano Process Equipments" of the Ministry of Knowledge Economy, Republic of Korea and supported by the IT R&D program of MKE/KEIT (2009-F-004-01, Technology Development of 30 nm level High Density Perpendicular STT-MRAM).

1) K. Suzuki *et al.*: Plasma Source Sci. Technol. **9** (2000) 199.
2) J. Keller *et al.*: J. Vac. Sci. Technol. A **11** (1993) 2487.
3) N. S. Yoon *et al.*: IEEE Trans. Plasma Sci. **26** (1998) 190.
4) H. Sugai *et al.*: Jpn. J. Appl. Phys. **33** (1994) 2189.
5) M. Kanoh *et al.*: Jpn. J. Appl. Phys. **40** (2001) 5419.
6) J. H. Lim *et al.*: J. Phys. D **42** (2009) 15204.
7) D. H. Kang *et al.*: Appl. Phys. Lett. **84** (2004) 3283.
8) V. A. Godyak *et al.*: Plasma Source Sci. Technol. **3** (1994) 169.
9) S. H. Seo *et al.*: Appl. Phys. Lett. **74** (1999) 2776.
10) J. Hopwood: Plasma Source Sci. Technol. **3** (1994) 460.
11) R. B. Piejak *et al.*: Plasma Source Sci. Technol. **1** (1992) 179.
12) K. N. Kim *et al.*: J. Appl. Phys. **97** (2005) 063302.